Long-range correlations induced by the self-regulation of zonal flows and drift-wave turbulence

P. Manz,[1,2] M. Ramisch,[3] and U. Stroth[3]

[1]*Center for Energy Research, University of California at San Diego, San Diego, California 92093, USA*

[2]*Center for Momentum Transport and Flow Organization, University of California at San Diego, San Diego, California 92093, USA*

[3]*Institut für Plasmaforschung, Universität Stuttgart, D-70569 Stuttgart, Germany*

By means of a unique probe array, the interaction between zonal flows and broad-band drift-wave turbulence has been investigated experimentally in a magnetized toroidal plasma. Homogeneous potential fluctuations on a magnetic flux surface, previously reported as long range correlations, could be traced back to a predator-prey-like interaction between the turbulence and the zonal flow. At higher frequency the nonlocal transfer of energy to the zonal flow is dominant and the low-frequency oscillations are shown to result from the reduced turbulence activity due to this energy loss. This self-regulation process turns out to be enhanced with increased background shear flows.

I. INTRODUCTION

The interaction between micro and macroscale turbulent fluctuations has developed into one of the most active research topics in the physics of magnetized plasmas. In toroidally confined plasmas, small scale turbulence can excite zonal flows (ZF), which are observed as stationary ($\omega=0$), azimuthally and toroidally homogeneous ($k_\theta=0$, $k_\phi=0$) and radially varying ($k_r \neq 0$) shear flows. Due to this structure, ZFs are unable to tap energy from the background profiles and therefore do not contribute to radial transport. In addition, since they are driven by the turbulent fluctuations through Reynolds stress, ZFs constitute an energy sink for the turbulence and therefore they can even cause transport reduction. Because of these properties, ZFs and their interactions with the ambient turbulence have been intensively studied in the last decade. The interested reader will be referred to a theory [1] and an experimental review [2] and a concise summary [3].

For an experimental identification of ZFs in toroidal plasmas, usually potential fluctuations measured at two distinct toroidal locations, which are not closely connected by a magnetic field line, are analyzed. A high level of coherence and a cross-phase close to zero between the two signals are interpreted as being caused by a potential structure, fluctuating homogeneously on the entire flux-surface. These long-range correlations therefore served as an indicator of ZFs in various experiments [4–6]. Recently, the observations of an amplification of such long-range correlation during the development of externally driven radial electric fields via electrode biasing have attracted attention [7–10]. Correlations are a result of fluctuating signals and cannot be explained by a mean (zero frequency) shear flow. This raises the important question of the physical mechanism behind these coherent fluctuations. Theoretically, two possible solutions have been put forward [3], the excitation of coherent geodesic acoustic modes (GAMs) by the ZF or a predator-prey-like interaction between the ZF and the broad-band turbulence.

Previous experimental investigations in magnetized plasmas mainly focus on the identification [4–10] or generation [11–15] of ZFs, mostly using measurements at only two points on a flux surface. In this work measurements in the stellarator experiment TJ-K [16] at 128 spatial locations are used to investigate the temporal behaviors and the correlation of both the ZF and the ambient drift-wave (DW) turbulence. In what follows, the analysis will be done for two situations, one where the plasma is unbiased and the other where a strong mean flow was induced by plasma biasing [17]. The biasing was used to reproduce the observation that long-range correlations are amplified in cases with stronger background flows. Without biasing, so far no strong ZF activity were found in TJ-K.

II. PREDATOR-PREY MODEL

Predator-prey oscillations are solutions of the Lotka-Volterra equations [18], which, e.g., play a fundamental role in theoretical biology to describe population dynamics. It has been shown in a simplified model [19] that the turbulent drift-wave enstrophy

$$\langle N \rangle = \sum_{k_\theta \neq 0, \ k_r \neq 0} N_{\mathbf{k}} = \sum_{k_\theta \neq 0, \ k_r \neq 0} (1 + (k\rho_s)^2)^2 |\phi_{\mathbf{k}}|^2 \quad (1)$$

and the zonal-flow enstrophy

$$U^2 = \sum_{k_\theta = 0, \ k_r \neq 0} (k_r \rho_s)^4 |\phi_{\mathbf{k}}|^2, \quad (2)$$

where $U = \partial V_{ZF} / \partial r$ is the shear of the zonal flow V_{ZF}, are exactly the two quantities which obey a predator (the ZF) prey (the DWs) relationship.

Zonal flows coexist with drift waves and form with them a self-regulating system. The drift waves grow by their own instability with the growth rate γ_L. Zonal flows are unable to tap energy from the background profiles themselves, thus, they cannot grow on their own, but they are damped with a damping rate γ_D, which is determined by, e.g., the ion-ion collisionality, geodesic transfer [20], and parallel viscosity. Therefore, they cannot persist without energy feed, which is provided by nonlinear interactions with the drift waves ($\sim U^2 \langle N \rangle$) accompanied by a damping of the turbulence ($\sim -U^2 \langle N \rangle$). Through this damping of the drift wave the growth

of the ZF is limited. Thus, the zonal flow—drift-wave system follows a predator-prey model [19]

$$\left(\frac{\partial}{\partial t} - \gamma_L\right)\langle N\rangle = -\alpha U^2 \langle N\rangle, \tag{3}$$

$$\left(\frac{\partial}{\partial t} + \gamma_D\right) U^2 = \beta U^2 \langle N\rangle. \tag{4}$$

Where the drift-wave enstrophy $\langle N\rangle$ corresponds to the prey, the zonal-flow enstrophy U^2 takes the role of the predator. The constants α and β are in fact differential operators. Thus, the predator-prey model is indeed a very oversimplified approach for the interaction of zonal flows and the ambient turbulence.

The predator-prey model exhibits two equilibrium states. The first trivial solution $(\langle N\rangle, U^2) = (0,0)$ describes the extinction of both "species," the second one is $(\langle N\rangle, U^2) = (\gamma_D/\alpha, \gamma_L/\beta)$. This system has a characteristic oscillation frequency at $\omega = \sqrt{\gamma_L\gamma_D}$. A consequence of this model is that the population of the predator follows that of the prey by $\pi/2$. Also this oversimplified picture of the zonal flow—drift-wave turbulence interaction scheme is very popular in the zonal-flow physics of fusion plasmas, and experimental evidence is still receivable.

III. EXPERIMENTAL SET UP AND PREVIOUS FINDINGS

To investigate the coupling between the macroscopic flow and the microscopic fluctuations, a wide range of spatial scales has to be resolved. This became possible with a massive probe system [9] in the stellarator experiment TJ-K [16]. TJ-K has major and minor radii of $R_0 = 0.6$ m and $a = 0.1$ m, respectively. It confines a low temperature plasma with dimensionless parameters similar to those in fusion edge plasmas [16]. The working gas used for the present experiments was helium at a neutral gas pressure of $p = 7$ mPa. The plasma had a line-averaged density of about $\bar{n} = 10^{17}$ m^{-3} and was generated by microwaves at a frequency of 2.45 GHz and a power of 1.8 kW at a magnetic field strength of $B = 72$ mT [21]. Temperature profiles are relatively flat. The electron temperature was about $T_e = 9$ eV and the ion temperature less than 1 eV. Density gradients are the main source of turbulent energy. Previous studies have shown that drift-waves are the dominant drive of the turbulence in TJ-K [16,22–25].

The moderate temperatures allowed for measurements of long time series (1 s at 1 MHz), which is an important factor for the statistical analysis presented in this work. The array consists of 128 Langmuir probes with 32 probes positioned on the poloidal circumferences of each of four neighboring flux surfaces. The array provides the inimitable possibility to measure on four entire flux surfaces simultaneously. This is necessary to unambiguously extract the ZF component ($k_\theta = 0$, $k_r \neq 0$) and to estimate its turbulent drive given by the radial derivative of the Reynolds stress (RS). To estimate the Reynolds stress $\langle \tilde{v}_r \tilde{v}_\theta \rangle_\theta$ one has to measure the radial and poloidal electric field simultaneously. Since the Reynolds stress is a flux-surface averaged quantity, many measure-
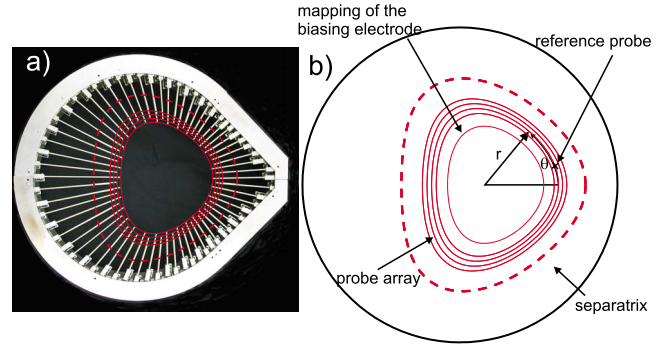
FIG. 1. (Color online) (a) Photo of the poloidal probe array. (b) Alignment of the probe array with respect to the biasing electrode on the flux surfaces of TJ-K. The dashed lines depict the separatrix (from Ref. [9]).

ments of potential fluctuations have to be done on two flux-surfaces. From the experimental data of the RS array, the zonal average is approximated by the poloidal one $\langle \cdot \rangle_\theta$. And because the turbulent drive is given by the radial derivative of the Reynold stress, measurements on four flux surfaces are needed to address this problem adequately. The poloidal and radial probe distances were 1.5 and 0.5 cm, respectively. The poloidal RS array is set up in a radial region of steep density gradients. Figure 1 shows the location of probes inside the plasma. The measured floating potential fluctuations are interpreted as plasma potential fluctuations $\tilde{\phi}$, which has been shown to be valid for TJ-K plasmas [26]. The measured potential fluctuations are normalized to the electron temperature, $\phi = e\tilde{\phi}/T_e$. In order to have the possibility to modify the shear flow, a biasing electrode in the shape of a flux surface inside the probe array has been installed (Fig. 1).

Basically the RS array provide two possibilities, which are beyond the means of common investigations. First scale resolved analyses can be done, where the time is used for the average. Second time resolved analyses can be carried out, where the flux-surface average is taken. This provides an observation closer to theory and more reliable results. Already the RS array has been used for scale resolved analyses identifying the turbulent drive of ZFs by an bispectral analysis method [15]. In previous investigations using bispectral analysis methods a nonlocal coupling between turbulence and ZFs including GAMs, has been demonstrated, e.g., in Refs. [4,27–30]. However, a bicoherence analysis yields information on the degree of phase locking of different modes only and, thus, identifies modes that can couple with each other. Driving or damping of ZFs and the relative importance of the various interactions can only be estimated from an energy transfer analysis. Energy transfer studies of the turbulence-ZF interaction and the turbulent cascades have been carried out [31–35]. These studies were done in frequency space, too, using Taylor hypothesis to transform the fluctuations from frequency to k-space. Furthermore, the analysis was done in one dimension only. The physical processes, however, take place in the two-dimensional wave number space [20]. There have been done only a few studies in k-space directly [36–38], considering the energy transfer among the different scales excluding the ZF. Using the RS
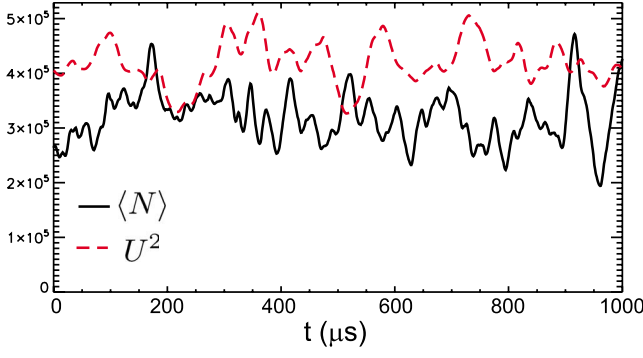
FIG. 2. (Color online) Time series of the drift-wave $\langle N \rangle$ (solid) and the zonal-flow enstrophy U^2 (dashed) in the unbiased case.

array the nonlinear energy transfer between the ZF and DW turbulence has been calculated directly in k space for the first time, showing an energetic drive of the ZF predominantly from the smaller scale turbulence $k\rho_s \gtrsim 1$ [15]. This is consistent with theory predicting that zonal flows are driven nonlocally in k-space by the parametric modulational instability [1]. From this picture one would expect that the energy comes predominantly from the larger scales, where most of the energy is located. But the energetic drive is highly nonlocal, consistent with drift-wave simulations [20] and recent observations in frequency space [39]. This can be understood by the straining-out process, where the eddies are tilted, elongated and finally curled up by the flow shear [15]. The straining-out process is most effective, if the vorticity and therefore the scales of the interacting flows are clearly different as in case of zonal flows and small-scale vortices. The staining-out process can also explain the non local energy transfer among the different scales concerning the inverse cascade [37]. In the present work the second possibility will be exploited. The probe configuration is used for the exact estimation of the flux surface average, which provides an accurate distinction of the ZF component ($k_\theta = 0$, $k_r \neq 0$) and the DW components ($k_\theta \neq 0$, $k_r \neq 0$) at every measured time point, to investigate their interplay and dynamics in detail.

IV. SELF-GENERATED SHEAR FLOWS

The data from the 2D probe array were analyzed in k-space directly. The multiprobe array allows to estimate the two-dimensional k-spectrum with high poloidal resolution $k_\theta \in \{-16, \ldots, 16\}[2\pi/(32 \times 0.015\rho_s)]$, whereas the radial resolution is poor $k_r \in \{-2, -1, 1, 2\}[2\pi/(4 \times 0.005\rho_s)]$. Here $\rho_s = \sqrt{m_i T_e}/eB$ is the drift scale parameter and m_i the ion mass. The simultaneous measurement of potential fluctuations at 128 positions provides the unique possibility to estimate the time series and the correlation between the turbulent drift-wave and the zonal-flow enstrophy.

Figure 2 shows time traces of the DW and the ZF enstrophy according to Eqs. (1) and (2), respectively. Both signals show irregular fluctuations and no sign of coherent modes such as GAMs. Although ZFs are not strongly pronounced in unbiased TJ-K plasmas, the interaction between a possible smaller ZF amplitude and DW turbulence is investigated. To this end, Fig. 3 shows the cross-correlation function between
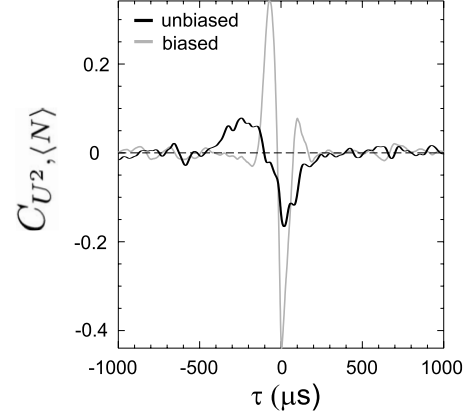
FIG. 3. Cross-correlation between the ZF U^2 and the DW enstrophy $\langle N \rangle$ with (gray) and without biasing (black).

the ZF enstrophy and the DW turbulent enstrophy,

$$C_{U^2,\langle N \rangle}(\tau) = \frac{\langle U^2(t)\langle N \rangle(t + \tau)\rangle_t}{\sigma_{U^2}\sigma_{\langle N \rangle}}, \quad (5)$$

where σ is the standard deviation of the zonal vorticity U^2 and the turbulent energy $\langle N \rangle$ and the brackets $\langle \cdot \rangle_t$ temporal averaging. The mean values of $U^2(t)$ and $\langle N \rangle(t)$ have to be subtracted before the cross-correlation is calculated. For zero time lag $\tau = 0$, a clear anticorrelation ($C_{U^2,\langle N \rangle} = -0.16$) is observed, indicating that the turbulent energy assumes a minimum when the excitation of the ZF is strongest. This observation is consistent with previous two-point measurements, using the low-frequency intensity as an indicator for the zonal-flow intensity [11–14], and with an analysis of drift-wave turbulence simulations [40]. The time lag of maximum anticorrelation is positive ($\tau \approx 20~\mu$s). Thus, when the ZF shear increases the energy in the turbulence decreases and vice versa. With the present analysis method the direction of the energy transfer cannot be resolved. In a previous investigation of the same discharge it has been shown that the energy is nonlinear transferred ($\sim U^2\langle N \rangle$) from the DWs (prey) to the ZF (predator) [15]. Thus, this is an energy loss and hence damping mechanism for the DWs. However, this alone is not a predator-prey oscillation. At negative time lags from -450 to $-100~\mu$s, the correlation function assumes small positive values, indicating a simultaneous increase in both ZF energy and turbulent drive. According to Ref. [41], the significance of the correlation, which gives the probability that this correlation is randomly generated, is given by $S = \text{erfc}(|C_{U^2,\langle N \rangle}|\sqrt{M/2})$, with erfc the complementary error function and M the number of averaged subwindows. Due to the high number of $M = 1000$ the small correlation level at $\tau \approx -250~\mu$s is still significant ($S = 3\%$). Through the energy transfer to the ZF and the corresponding damping of the DWs the growth of the ZF is limited. A consequence of this model is that the population of the predator follows that of the prey by $\pi/2$. This is consistent with Fig. 3, where the ZF is following the DW enstrophy, which can been seen in the positive correlation at nonvanishing time lag. The detailed temporal sequence of an excitation of the ZF by DW turbulence followed by a saturation due to the loss of DW energy
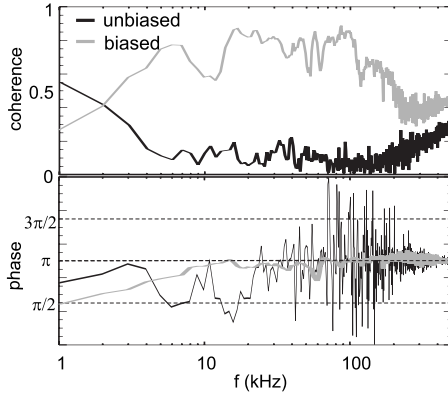
FIG. 4. Cross-coherence and -phase between the ZF U^2 and the DW enstrophy $\langle N \rangle$ with (gray) and without biasing (black). The α =95% confidence limit for the coherence is given by $1-(1-\alpha)^{1/(M-1)} \approx 0.003$ [44].

is observed for the first time and goes beyond previous investigations [11–14].

To verify the predicted cross-phase of $\pi/2$ a cross-coherence analysis is presented in Fig. 4. The averaged cross-power spectrum is given by

$$H_{\langle N \rangle, U^2}(\omega) = \langle \langle N \rangle^*(\omega) U^2(\omega) \rangle, \quad (6)$$

where $\langle N \rangle(\omega)$ and $U^2(\omega)$ are the Fourier transforms in time of $\langle N \rangle(t)$ and $U^2(t)$ taking 1000 subseries of 1024 points for ensemble averaging $\langle \cdot \rangle$. As a complex quantity, the cross-power spectrum can be written as $H_{\langle N \rangle, U^2}(\omega)$ $= |H_{\langle N \rangle, U^2}(\omega)| e^{i\varphi_{\langle N \rangle, U^2}(\omega)}$, where $\varphi_{\langle N \rangle, U^2}(\omega)$ is the average cross-phase. The coherence, defined by

$$\gamma_{\langle N \rangle, U^2}(\omega) = \frac{|\langle \langle N \rangle^*(\omega) U^2(\omega) \rangle|}{\sqrt{\langle |\langle N \rangle(\omega)|\rangle^2 \langle |U^2(\omega)|\rangle^2}}, \quad (7)$$

measures, how phase locked modes are with values in [0,1]. Significant coherence can be found only in the low-frequency range 1–3 kHz where the cross-phase ranges between π and $\pi/2$. A cross-phase of π indicates energy transfer between turbulence and zonal flow but a clear evidence for the predator-prey cycle cannot be deduced from these data. For $f > 3$ kHz, the coherence is very low leading to a large scatter in the cross-phases. But the energy can be transferred between the turbulence and the ZF if the cross-phase is between $\pi/2$ and $3\pi/2$, which is fulfilled nearly for all frequencies.

The reason for the absence of strong ZF activity in unbiased TJ-K discharges can be found in the relatively high collisionality of these plasmas. It has been shown [36] that due to the moderate adiabaticity, the nonlinear dynamics of potential and density fluctuations is quite different. In addition to the increased collisional damping of the ZF, this obstructs the self-amplification mechanism. The Reynolds stress process requires an adiabatic coupling between potential and pressure perturbations, since the zonal flow directly tilts the pressure but not the potential perturbations [20].
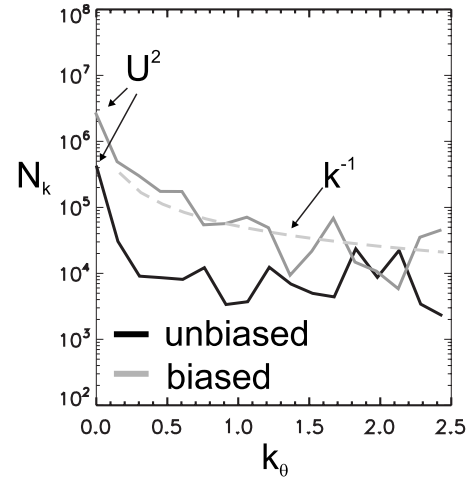
FIG. 5. Drift-wave enstrophy spectra $\Sigma_{k_r \neq 0} N_{\mathbf{k}}$ with and without biasing. Contributions to the zonal-flow enstrophy U^2 can be found at $k_\theta = 0$.

Only for adiabatic electrons, the potential can follow the tilt of the density fluctuations, which in turn results in an energy transfer to the zonal flow [20].

V. INFLUENCE OF AN EXTERNAL SHEAR FLOW

In order to be able to investigate the ZF-DW interaction in the background of large amplitude flows, plasma biasing has been applied. Details on the plasma biasing scenario can be found in Ref. [17]. Previous studies [9] showed that biasing is efficient to excite mean flows ($m=0$) with a strong fluctuating component at low frequencies (≈ 1 kHz). Furthermore, it has been shown that the correlation of the flux-surface averaged zonal shear flow and the Reynolds stress is strongly enhanced during biasing, indicating a strong energy transfer from the turbulence to the zonal flow [42]. Hence, equilibrium shear flows could initiate an anisotropy in the velocity fluctuations by tilting vortices and serve as a trigger for turbulence-driven ZFs. At the position of the probe array due to biasing the plasma density and also the collisionality decreases by an order of magnitude. This could be responsible for the observed excitation of the $m=0$ component. Also the enstrophy k-spectra summed up over $k_r \neq 0$ shown in Fig. 5 show the amplification of the ZF component during biasing. Furthermore without biasing the enstrophy spectrum is nearly constant corresponding to an energy spectrum $E \sim k^{-\alpha}$ with α around 2. During biasing the enstrophy undergoes a transition to a spectrum close to k^{-1} with a corresponding energy spectrum $E \sim k^{-3}$, which is consistent with the spectral condensation resulting in large scale coherent flows as ZFs [43]. Figure 6 depicts the frequency spectra of the ZF and the DW enstrophy under biasing. Again no sign of a coherent GAM is found in the ZF spectrum. The peak in the DW spectrum at 56 kHz can be traced to a quasicoherent $m=3$ mode according to Ref. [9]. Hence, the previously observed ZF oscillations might be a signature of predator-prey cycles.

The cross-correlation function (Fig. 3) exhibits the same features as without biasing, however, now at much higher
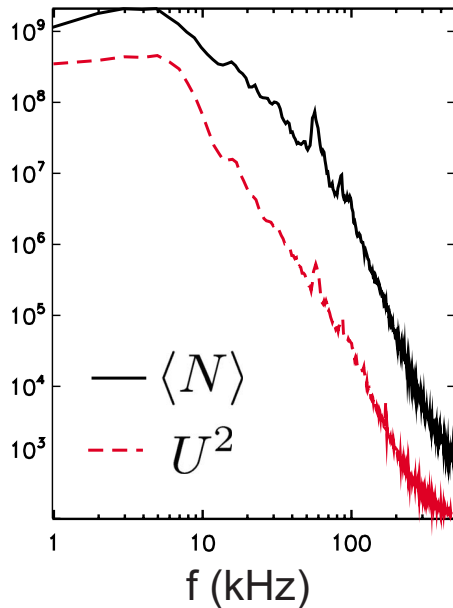
FIG. 6. (Color online) Spectra of the DW turbulent energy $\langle N \rangle$ (solid) and the ZF enstrophy U^2 (dashed) during biasing.

correlation. Hence, the energy transfer between the turbulence and the zonal shear flow is clearly enhanced. The corresponding coherence analysis, shown in Fig. 4, now yields rather high values of above 0.5 in the range between 10 and 100 kHz. The cross-phase is nearly constant at about π consistent with a nonlocal, nonlinear energy transfer from DW turbulence to the ZF as also reported previously in Refs. [15,39]. Here nonlocal means that the involved spectral scales are separated by more than a factor of two. At lower frequencies ≈ 1 kHz, a cross-phase of $\pi/2$ if found, indicating predator-prey oscillations. Also at this low coherence $\gamma_{U^2,\langle N \rangle} \approx 0.25$ the number of realizations $M = 1000$ ensure a small error in the phase estimation $\pm 1.96[(2M)^{-1}(\gamma_{U^2,\langle N \rangle}^{-1} - 1)] \approx 0.003$ [44]. Therefore, the oscillatory behavior of the ZF-like structures in the 1 kHz range can be explained by the self-regulation of the system. On the other hand by approximating ZFs by the low-frequency intensities, as done in Refs.

[11–14], predator-prey oscillations cannot be observed directly, since the correlation between the ZF and low-frequency DW intensities cannot be resolved.

In Ref. [31], the correlation between turbulence and geodesic acoustic oscillations has been investigated. A cross-phase close to $\pi/2$ was found as consistent with the basic predator-prey model. But the sign of the correlation was opposite indicating that the GAM leads to the turbulence [31]. The authors concluded that nonlinear damping of the GAM is responsible for the opposite sign [31]. However, due to the geodesic transfer [20] the energy of the ZF and the GAM is anticorrelated, which leads to an additional phase shift of π. Hence, it makes indeed a difference whether ZFs or GAMs are considered in such an investigation.

VI. CONCLUSION

In summary, the energetic interaction between the zonal flows and the drift-wave turbulence has been investigated experimentally. Using a massive probe array, fluctuations have been measured in unprecedent spatial resolution to estimate the flux surface-averaged drift-wave and zonal-flow enstrophy. Long time series with high resolution allowed for significant statistical analyses. Two elements of a predator-prey-like interaction could be identified: (i) the energy transfer from the DW turbulence to the ZF is indicated by a cross-phase of π between the two quantities at higher frequencies. As shown previously [15], this transfer is nonlocal, i.e., the energy comes from the smaller scales. (ii) at frequencies ≈ 1 kHz a cross-phase of $\pi/2$ with a coherence >0.25 is consistent with the predator-prey model [19]. In TJ-K this element becomes only significant when the background flow is enhanced, but it could also be triggered by spontaneous confinement transitions. Hence, the long-range correlations in the potential fluctuations as observed in Refs. [4–8,10–14] are likely to be predator-prey oscillations, too.

[1] P. H. Diamond *et al.*, Plasma Phys. Controlled Fusion **47**, R35 (2005).

[2] A. Fujisawa *et al.*, Nucl. Fusion **49**, 013001 (2009).

[3] K. Itoh, K. Hallatschek, and S.-I. Itoh, Plasma Phys. Controlled Fusion **47**, 451 (2005).

[4] G. S. Xu, B. N. Wan, M. Song, and J. Li, Phys. Rev. Lett. **91**, 125001 (2003).

[5] A. Fujisawa *et al.*, Phys. Rev. Lett. **93**, 165002 (2004).

[6] D. K. Gupta, R. J. Fonck, G. R. McKee, D. J. Schlossberg, and M. W. Shafer, Phys. Rev. Lett. **97**, 125002 (2006).

[7] M. A. Pedrosa, C. Silva, C. Hidalgo, B. A. Carreras, R. O. Orozco, and D. Carralero (TJ-IIteam), Phys. Rev. Lett. **100**, 215003 (2008).

[8] C. Silva *et al.*, Phys. Plasmas **15**, 120703 (2008).

[9] P. Manz, M. Ramisch, and U. Stroth, Phys. Plasmas **16**, 042309 (2009).

[10] Y. Xu *et al.*, Phys. Plasmas **16**, 110704 (2009).

[11] A. Fujisawa *et al.*, Plasma Phys. Controlled Fusion **48**, A365 (2006).

[12] C. Hidalgo *et al.*, EPL **87**, 55002 (2009).

[13] A. D. Liu *et al.*, Phys. Rev. Lett. **103**, 095002 (2009).

[14] Z. Yan *et al.*, Phys. Plasmas **17**, 032302 (2010).

[15] P. Manz, M. Ramisch, and U. Stroth, Phys. Rev. Lett. **103**, 165004 (2009).

[16] U. Stroth *et al.*, Phys. Plasmas **11**, 2558 (2004).

[17] M. Ramisch *et al.*, Plasma Phys. Controlled Fusion **49**, 777 (2007).

[18] V. Volterra, Nature (London) **118**, 558 (1926).

[19] P. H. Diamond *et al.*, *Proceedings of the 17th IAEA Fusion Energy Conference*, Yokohama, Japan IAEA CN69/TH3/1 (IAEA, Vienna, 1998).

[20] B. D. Scott, New J. Phys. **7**, 92 (2005).

[21] A. Köhn *et al.*, Plasma Phys. Controlled Fusion **52**, 035003 (2010).

[22] M. Ramisch *et al.*, Phys. Plasmas **12**, 032504 (2005).

[23] N. Mahdizadeh *et al.*, Plasma Phys. Controlled Fusion **49**, 1005 (2007).

[24] M. Ramisch *et al.*, Plasma Sources Sci. Technol. **17**, 024007 (2008).

[25] K. Rahbarnia *et al.*, Plasma Phys. Controlled Fusion **50**, 085008 (2008).

[26] N. Mahdizadeh *et al.*, Plasma Phys. Controlled Fusion **47**, 569 (2005).

[27] Y. Nagashima *et al.*, Phys. Rev. Lett. **95**, 095002 (2005).

[28] K. J. Zhao *et al.*, Phys. Rev. Lett. **96**, 255004 (2006).

[29] A. Fujisawa *et al.*, Plasma Phys. Controlled Fusion **49**, 211 (2007).

[30] R. A. Moyer, G. R. Tynan, C. Holland, and M. J. Burin, Phys. Rev. Lett. **87**, 135001 (2001).

[31] C. Holland *et al.*, Phys. Plasmas **14**, 056112 (2007).

[32] Y. Nagashima *et al.*, Phys. Plasmas **16**, 020706 (2009).

[33] H. Xia and M. G. Shats, Phys. Rev. Lett. **91**, 155001 (2003).

[34] H. Xia and M. G. Shats, Phys. Plasmas **11**, 561 (2004).

[35] M. Xu *et al.*, Phys. Plasmas **16**, 042312 (2009).

[36] P. Manz *et al.*, Plasma Phys. Controlled Fusion **50**, 035008 (2008).

[37] P. Manz, M. Ramisch, and U. Stroth, Plasma Phys. Controlled Fusion **51**, 035008 (2009).

[38] T. Yamada *et al.*, Phys. Plasmas **17**, 052313 (2010).

[39] M. Xu *et al.*, Phys. Plasmas **17**, 032311 (2010).

[40] M. Ramisch *et al.*, New J. Phys. **5**, 12 (2003).

[41] W. H. Press *et al.*, *Numerical Recipes in FORTRAN 77* (Cambridge University Press, Cambridge, England, 1992).

[42] M. Ramisch *et al.*, Contrib. Plasma Phys. **50**, 718 (2010).

[43] M. G. Shats, H. Xia, and H. Punzmann, Phys. Rev. E **71**, 046409 (2005).

[44] D. M. Halliday *et al.*, Prog. Biophys. Mol. Biol. **64**, 237 (1995).